WATER RESOURCES RESEARCH, VOL. 27, NO. 12, PAGES 3065–3073, DECEMBER 1991

Effect of Catchment-Scale Subsurface Mixing on Stream Isotopic Response

J. J. McDONNELL

Watershed Science Unit, Department of Forest Resources, Utah State University, Logan

M. K. STEWART

Institute of Nuclear Sciences, Department of Scientific and Industrial Research, Lower Hutt, New Zealand

I. F. OWENS

Department of Geography, University of Canterbury, Christchurch, New Zealand

A 3.8-ha watershed on the west coast of New Zealand was instrumented with suction lysimeters and automatic water samplers to determine the relationship between subsurface isotopic and chemical concentrations to those of rainfall and resulting streamflow. A t test showed that ±2‰ represented a significant difference between successive sample deuterium values. Eleven rainfall episodes were subdivided into two categories: (1) two events where stream isotopic composition did not deflect >2‰ from prestorm values, and (2) four events which demonstrated new water flushing. Detailed analysis of one 47-mm rainfall (9.8-mm runoff) event showed that old water dominated streamwater exiting the watershed by 90% using a standard two-component hydrograph separation for deuterium (corroborated by Cl and electrical conductivity). Three-component hydrograph separation indicated that 12–16% was in the form of soil water, with <5% as on-channel precipitation and 80% groundwater. Analysis of over 1000 water samples revealed systematic trends in soil water and groundwater isotopic composition both in a downslope and downprofile direction. Between-storm suction lysimeter deuterium data showed a systematic dampened response to temporally variable rainfall deuterium concentrations. Multivariate cluster analysis revealed three distinct soil water/groundwater groupings, with respect to soil depth and geographic position within the watershed. Within-storm suction lysimeter sampling preserved similar groupings, indicating that the subsurface reservoir is poorly mixed on short time scales. Understanding subsurface mixing response to rainfall should greatly improve models of episodic stream response and partitioning of storm flow into waters of different age.

INTRODUCTION

Environmental problems such as acidic deposition have adverse effects on the chemistry of streams and lakes over the long term, and much study has been done in determining the causes and consequences of chronic long-term acidification. Recent study of short-term rainfall events [*Seip et al.*, 1989], however, has shown that "episodes" may be of greater importance than sustained low-level acidification because even relatively brief adverse changes in surface water chemistry can have significant adverse long-term effects on aquatic biota. Although in-stream and near-stream hydrologic processes have recently been related to episodic response [e.g., *Pionke et al.*, 1988], hillslope hydrologic processes, both within and between events, may also greatly control episodic response of streams. This is particularly true for steep humid headwater catchments, where subsurface storm flow and routing into hillslope hollows predominates. In some studies, conservative isotopic tracing has been performed to characterize the various components contributing to stream episodic response. Because isotopic tracers are conservative, they are ideal for relating flow pathways and water residence time to in-stream response. The tracer concentrations of soil water, groundwater and streamflow are generally interpreted using a two-component mass balance. Isotope concentrations of water samples are expressed as per mil (‰) differences relative to the international standard, SMOW (standard mean ocean water) as defined by *Craig* [1961]. A two-component separation model [*Pearce et al.*, 1986]:

$$Q_n = Q_t - Q_o \tag{1}$$

$$Q_o = [(C_t - C_n)/(C_o - C_n)]Q_t \tag{2}$$

is used, where Q_t, Q_o and Q_n represent current streamflow, old water (stored subsurface water, including soil water (vadose) and groundwater (phreatic)), and new water (rainfall) volumes respectively, and C_t, C_o and C_n are the corresponding tracer concentrations. A three-component tracer model [*DeWalle et al.*, 1988] has also been used to include soil water as a separate component, where

$$Q_t = Q_{cp} + Q_s + Q_{gw} \tag{3}$$

$$Q_s/Q_t = [(C_t - C_{gw})/(C_s - C_{gw})] - Q_{cp}/Q_t[(C_{cp} - C_{gw})/(C_s - C_{gw})] \tag{4}$$

where subscripts s, t, gw and cp represent soil water, current streamflow, groundwater and channel precipitation inputs, respectively. The objectives the present study are to (1) examine the spatial and temporal variability of soil water and groundwater deuterium concentration, both within and between events; (2) determine the hydrograph components for a number of rainfall episodes based on two- and three-component mass balance separations; and (3) comment on

Paper number 91WR02025.
0043-1397/91/91WR-02025$05.00

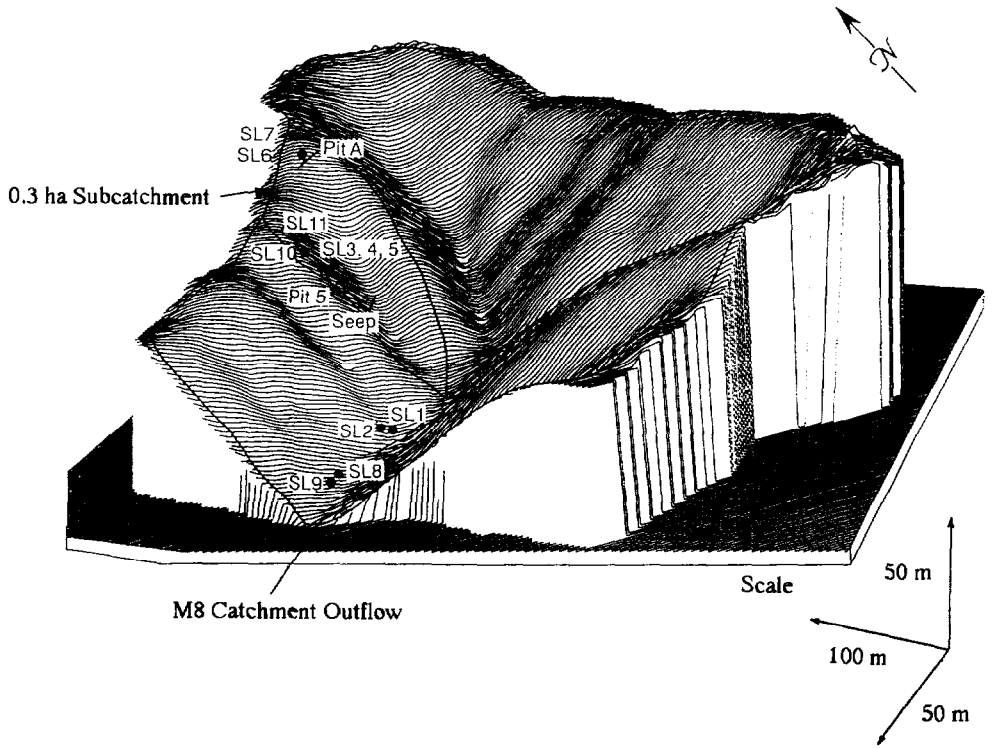

Fig. 1. Three-dimensional graphical representation of the M8 catchment showing suction lysimeter and throughflow and catchment outflow sampling points.

the applicability of isotope tracing in the Maimai watershed, particularly in light of measurement and sampling error.

This paper will show that although useful in some respects, two- and three-component separations are problematic for the Maimai M8 catchment and possibly other steep, humid catchments. This is because they attempt to relate dynamic stream response to static rainfall, soil water and groundwater conditions. Whereas *McDonnell et al.* [1990] have demonstrated the effect of varying rainfall isotopic composition on the validity of old water/new water estimates, this paper will demonstrate that one cannot assume static soil water or groundwater conditions in a steep catchment. Soil water and groundwater deuterium concentrations shift markedly, in time and space (C_n or $C_{cp} \ggg C_s > C_{gw}$) and also between and within storm events.

STUDY AREA AND METHODOLOGY

The M8 catchment is located on the South Island of New Zealand. Catchment hydrology and soils have been described by *Mosley* [1979], *Pearce et al.* [1986], and *McDonnell* [1990]. Briefly, the watershed is 3.8 ha in area, with 30°–40°, highly incised sideslopes. Soils (podzolized to mottled yellow brown earths) are generally less than 1 m thick, and overlie a firmly compacted conglomerate, known as the Old Man Gravels. Annual rainfall is evenly distributed, of the order of 2600 mm. Vegetation consists of regrowth *Pinus Radiata*, following a 1980 harvesting of the native beech and podocarp forest cover.

A three-dimensional graphical representation of the watershed is shown in Figure 1, and illustrates the water sampling locations within the main catchment and 0.3-ha subcatchment. Eleven Soil Moisture Corporation Model 1900 soil water samplers (suction lysimeters) were deployed in various topographic positions. Fifty to 85 cbar of suction was applied to each sampler, with samples collected at hourly, daily and weekly intervals. High humidity and wet soils resulted in negligible isotopic fractionation of the weekly samples. Streamflow was sampled at the catchment outflow using an automatic liquid sampler. In addition, throughflow was monitored in three slope positions (pit A, pit 5 and seep; Figure 1) by routing flow from a soil face into 210-L drums fitted with mini 10:1 V notch weirs and automatic liquid samplers. The pit construction was originally described by *Mosley* [1979], and later by *Sklash et al.* [1986] and *McDonnell* [1990]. Pit A represents an upslope hollow site (zero-order basin), approximately 10 m from the catchment divide. The longitudinal slope of the hollow is roughly 40°, while sideslopes into the hollow are 15°. Pit 5 represents a mid-slope hollow site, where soil depths and hollow sideslopes are greater. This site maintains a highly concave longitudinal and sideslope profile. The seep site represents a downslope hollow, where slopes are steeper and soils are shallow (0.3 m). Outflow from the seep flows directly into an incised first-order channel, draining the subcatchment.

Rain samples were collected sequentially within the catchment at 2.5 mm, 5 mm, and then successive 9.2-mm increments, using a method described by *McDonnell et al.* [1990]. Sampling accuracy was verified using a colocated tipping bucket rain gauge. Environmental isotope analyses were conducted at the Institute of Nuclear Sciences, Lower Hutt. Deuterium samples were prepared by the zinc reduction method [*Coleman et al.*, 1982] and analyses run on a V. G. Micromass 602 mass spectrometer. Deuterium samples were sealed in 30-mL bottles to prevent evaporation and resulting

isotopic fractionation. Solute chemistry analyses were conducted at the Forest Research Institute, Christchurch. Electrical conductivity (EC) was measured in the laboratory and in the field using portable Metrohm and pHox conductivity meters. Chloride (Cl) was analyzed using an automated mercuric thiocyanate-ferric nitrate method [*American Public Health Association*, 1976]. EC and Cl samples were stored in 250-mL bottles and cooled or frozen until time of analyses.

RESULTS

Water Sampling Considerations

Assuming that there is sufficient difference between prestorm streamflow and rainfall δD values, individual sample error in a short stream hydrograph time series is important to consider. This relates specifically to the significance of differences between prestorm δD and succeeding channel storm flow δD values. Replicate δD samples were run to determine machine experimental accuracy. Repeats of five sample groups showed that on any individual measurement, average standard deviation (s.d.) equals $\pm 1‰$ at the 0.05 level (i.e., 68% of the normally distributed data lie within $\pm 1‰$). Prestorm streamflow δD for each event was determined and then plotted within a $\pm 1‰$ error band through succeeding channel storm flow samples. An example of this technique is shown for a hypothetical event in Figure 2. After a prestorm stream δD of $-40‰$, an error band is projected through the event, whereby succeeding storm flow values fall either within or outside of this range. Those storm flow values within the range would be considered identical to prestorm δD. Values outside this range would also be plotted within a $\pm 1‰$ error band. If this overlapped with the prestorm δD error band, then the difference would be considered insignificant.

To quantify the arbitrary test described above, a t test was performed using artificial channel storm flow values compared with the prestorm stream δD:

$$t = (x_p - x_a)/(\mathrm{SE}(x_p - x_a)) \tag{5}$$

where t is the Student's test value compared with standard tables, x_p and x_a are sample mean of the prestorm and artificial variable δD respectively, and SE is the standard error of the difference between x_p and x_a. At the 0.05 level, $\pm 2‰$ represents the critical level for significant difference between prestorm stream and channel storm flow δD values.

Water was sampled from the M8 weir pool (located at the catchment outflow) because stream points immediately upstream and downstream were too shallow for intake hose placement. Similarly, throughflow from pits A and 5 and the seep into the 210-L storage drums was sampled from the drum reservoir, because of the low intermittent flows involved. Water automatically sampled from shallow reservoirs at set time intervals may be altered isotopically by its residence time within the pool. Theoretical pool flushing time (FT) was computed to determine isotopic mixing as a function of weir or drum outflow:

$$\mathrm{FT} = \mathrm{VOL}_{\mathrm{pool}}/\mathrm{VFR}_{\mathrm{out}} \tag{6}$$

where $\mathrm{VOL}_{\mathrm{pool}}$ is the weir or drum pool volume (cubic meters) and $\mathrm{VFR}_{\mathrm{out}}$ is the weir or drum volumetric flow rate (cubic meters per hour) assuming that the drums behave as continuously stirred tank reactors (CSTRs).

Figure 3*a* shows an exponential fit of equation (5) for the M8 weir. For low stage heights (<40–50 mm), computed flushing rate is very long (~10–20 hours), which would significantly alter the true isotopic composition of the streamflow. Fortunately, a stage of 40–50 mm represented a base flow condition within the M8 catchment (during the August to December 1987 period) and storm flow exceeded this value in every case within the first 30 min of flow. Because water samples were extracted from the weir pool on a 2- and 4-hour basis, storm hydrograph separation using these samples is considered accurate. A theoretical flushing curve for the 210-L drum is shown in Figure 3*b*. Most flow events started from an initial stage of 0–2 mm; therefore initial flushing was extremely slow (zero to 36 days), resulting in substantial error during the early stages of storm hydrograph rise. For the 4- and 8-hour sampling strategy used for drum samples, stage heights of 24 and 18 mm were required to limit flushing-induced errors to 0.5 times the sampling interval for 4- and 8-hour sampling respectively. Although the large drum size contributed some error at low

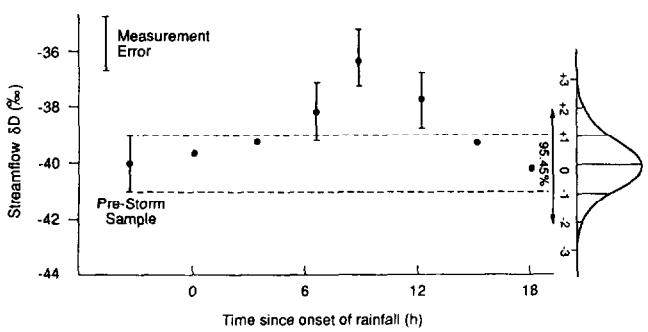

Fig. 2. Hypothetical storm event showing the effect of machine error on instantaneous samples within a channel storm flow δD time series.

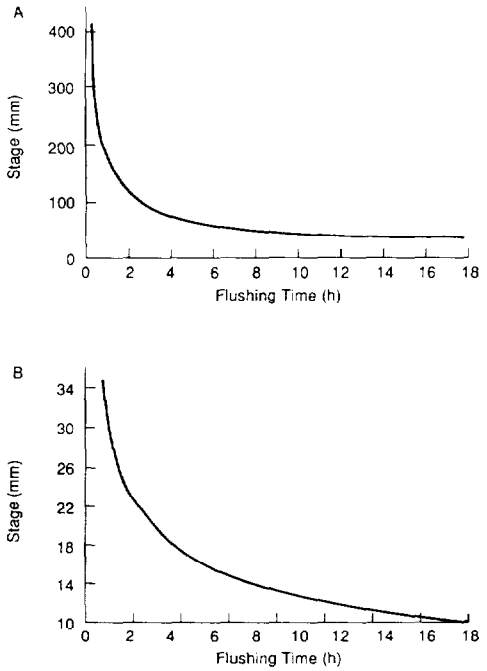

Fig. 3. Flushing rates for (*a*) M8 weir pool and (*b*) 210-L drums.

TABLE 1. Drum Flushing Experiment Results

Date	Time, LT	Drum δD, ‰	Hose δD, ‰	Difference, ‰
		Pit 5		
Nov. 27	1600	−37.7	−39.5	1.8
Nov. 29	1000	−40.2	−40.1	0.1
Dec. 2	1715	−39.1	−38.5	0.6
		Pit A		
Nov. 27	1600	−43.2	−40.3	2.9
Nov. 29	1000	−39.9	−41.8	1.9
Dec. 2	1715	−39.4	−39.3	0.1

flow, the reservoir could not be reduced in size because high-flow episodes occasionally matched the capacity of the drum and mini V notch weir assembly.

As an example of the time-flushing relationship, Table 1 shows δD differences for drum outflow versus hose input for varying flow stage relationships sampled during the November 26–28 event (discussed later in this paper). For the pit 5 outflow, drum water was −1.8‰ lighter than the input hose (i.e., true pitflow δD) at 1600 LT on November 27. Proceeding through the event, drum and hose δD were equal (±0.1‰) at 1000 LT on November 29. By 1715 LT on December 2, drum water was again approximately equal (±0.6‰) to hose water. Pit A drum water was −2.9‰ heavier than input water at 1600 LT on November 27. At 1000 LT on November 29, drum water was lighter than the input by −1.9‰ and then approximately equal to the input value ±0.1‰ by 1715 LT on December 2.

Stream Isotopic Response

Storm streamflow δD results from 11 episodes during a 4-month period in 1987 were subdivided into the three categories, according to their streamflow δD deflection away from prestorm δD. Five events occurred where weighted mean rain δD equaled prestorm streamflow δD (category 1). They are not discussed since isotopic hydrograph separation could not be accomplished. The other two groups comprise (1) two events where the stream showed no new water flushing (i.e., stream δD within the error band), and (2) four events where new water flushing was detectable.

The October 10 and November 13 events showed no detectable new water input into the stream channel. Rainfall and prestorm flow conditions are given in Table 2. Although each event showed large differences between rain δD and prestorm M8 δD (i.e., making them suitable for isotopic analysis), stream δD did not deflect away from the prestorm δD value (see Figure 4*e*). Thirty-four millimeters of rain fell in two distinct bursts in the November 13 example (Figure 4*a*). Streamflow and pit throughflow responded rapidly to 8–10 mm h^{-1} peak 10-min rainfall intensities. Peak catchment runoff was 1.05 mm h^{-1}, while pit A and pit 5 peaked at 3000 and 500 mL min^{-1}, respectively. Pit A peak coincided with M8 peak flow, but pit 5 peak flow occurred after a second small rainfall burst at 1300 LT on October 11. M8

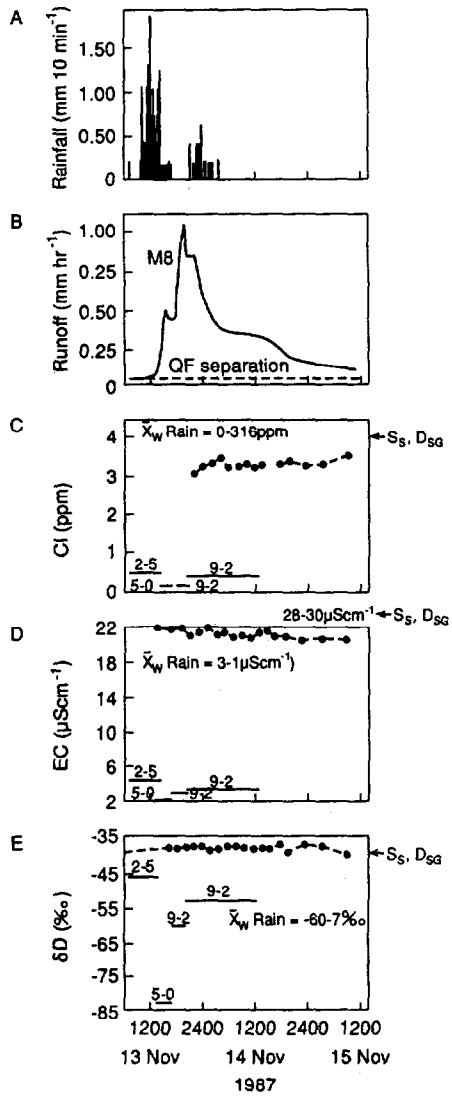

Fig. 4. Water volume, chloride, electrical conductivity and deuterium relationships for the 13 November 13 event. S_S and D_{SG} represent average shallow soil water and deep soil water and groundwater concentrations, respectively. Rainfall concentrations are shown as bars, with rain depths plotted above lines. See text for explanation of individual charts.

TABLE 2. Rainfall and Prestorm Conditions for Events With No Detectable New Water Input

Event	Rain, mm	API_7, mm	API_{14}, mm	QF/*R*, %	QF/*P*, %	$\delta\bar{x}_w$ Rain Cl, ppm	$\delta\bar{x}_w$ Rain EC, μS cm^{-1}	$\delta\bar{x}_w$ Rain δD, ‰	Prestorm M8 Cl, ppm	Prestorm M8 EC, μS cm^{-1}	Prestorm M8 δD, ‰
Oct. 10	43	31.2	33.6	48	37	2.67	12.9	−20.7	3.80	17.0	−37
Nov. 13	34	4.1	6.1	83	39	0.32	3.1	−60.7	3.40	21.5	−38

$API_7 = \Sigma_{i=1}^{7} P_i/i$ where API_7 is the 7-day antecedent precipitation index and P_i is the total gross precipitation on the *i*th day beforehand; QF is quick flow; *R* is runoff; *P* is storm precipitation total; and $\delta\bar{x}_w$ Rain is the weighted mean rainfall concentration.

TABLE 3. Rainfall and Prestorm Conditions for Events With Detectable New Water Input

Event	Rain, mm	API_7, mm	API_{14}, mm	QF/R, %	QF/P, %	δx_w Rain Cl, ppm	δx_w Rain EC, $\mu S\ cm^{-1}$	δx_w Rain δD, ‰	Prestorm M8 Cl, ppm	Prestorm M8 EC, $\mu S\ cm^{-1}$	Prestorm M8 δD, ‰
Sept. 30	26	1.5	4.1	80	44	3.60	14.6	−11.1	4.00	17.0	−39*
Oct. 7	65	4.7	6.2	85	45	2.63	9.7	−24.3	4.20	19.5	−39†
Oct. 13	103	35.1	37.5	80	62	2.84	4.4	−58.3	3.70	17.4	−39
Nov. 26	48	1.5	4.1	93	19	1.27	8.1	−65.8	4.00	23.0	−39

*Estimated sample from long-term base flow δD series.
†From sample at 0520 LT on October 2 in long-term base flow δD series.

was sampled at 2-hour intervals, but pit throughflow samples were not obtained for this event. Rainfall showed considerable isotopic variability, but remained lighter than prestorm M8 δD for the complete duration (weighted mean rainfall concentration, $\delta x_w = -60.7‰$) where:

$$\delta x_w = \sum_{i=1}^{n} P_i \delta_i \Big/ \sum_{i=1}^{n} P_i \qquad (7)$$

and where P_i and δi denote fractionately collected precipitation amount and deuterium concentration, respectively. M8 showed no detectable δD shift from a prestorm δD of −39.7‰. M8 Cl and EC concentrations also showed no response during the event, and reinforce the interpretation that for this storm, only a very small amount of the rainfall which fell directly on to the stream contributed to M8 storm streamflow.

Four events showed detectable new water input to the storm hydrograph and are listed in Table 3. The November 26–27 event is discussed. A total of 47 mm of precipitation (P) fell in two separate bursts on November 26 and 27. Peak 10-min rainfall intensities in each burst reached ~13 mm h^{-1}, but average intensities were <3 mm h^{-1} (Figure 5). Only 9.8 mm of measured runoff (R) at the weir was produced because of low antecedent wetness conditions (Table 2). M8 stream hydrograph response was bimodal and peaked at 0.40 mm h^{-1} at 1800 LT on November 26 and 0.68 mm h^{-1} at 0900 LT on November 27. Approximately 9 mm of quick flow (QF) was produced, but QF/P was <20%. The low QF/P value is due partly to the fact that the QF

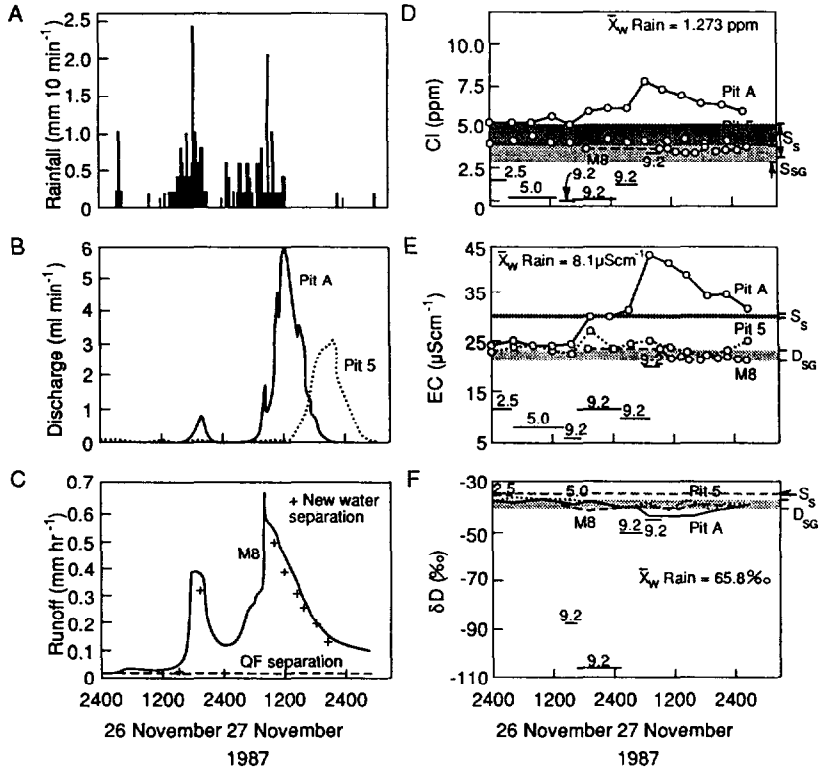

Fig. 5. Water volume, chloride, electrical conductivity and deuterium relationships for the November 26–27 event. S_S and D_{SG} represent average shallow soil water and deep soil water and groundwater concentrations, respectively. Rainfall concentrations shown as bars, with rain depths plotted above lines. Shaded horizontal strips indicate range in values. See text for explanation of individual charts.

TABLE 4. Suction Lysimeter Depths, Locations and Phenogram Groupings

SL	Depth, mm	Distance to Channel, m	Distance to Divide, m	Beween-Storm Grouping	Within-Storm Grouping
1	400	5	65	...	...
2	800	5	65	...	B
3	800	30	40	A	A
4	200	30	40	C	C
5	400	30	40	A	A
6	400	25	15	A	A
7	300	35	5	C	C
8	400	1	75	B	B
9	800	1	75	B	A
10	400	40	25	A	A
11	800	40	25	B	B

Letters designating groupings are discussed in text.

separation line [*Hewlett and Hibbert*, 1976] did not intersect the hydrograph receding limb by the end of the event at 0600 LT on November 28. The event was arbitrarily terminated at this point because another rain event commenced at 0700 LT, producing a separate storm runoff response. The events were separated because a >24 hour interval separated major rainfall bursts.

Rain δD fluctuated over 70‰, but this variation (except for the first 7.5 mm) occurred in the −45 to −105‰ range, with a weighted mean of −65.8‰. Although M8 showed evidence of some new water input for many of the collected water samples (Figure 5), each was <10%. Using a two-component separation (equation (2)), peak new water input (8%) occurred during the first hydrograph peak. The second hydrograph peak showed only 4% new water. Employing the three-component model (equation (4)), "soil water" averaged 12–16% near the crest of both hydrographs (Figure 5), while new water channel precipitation was <5% and groundwater approximately 80%.

M8 water chemistry showed little variation through the event and supports the δD interpretation of only a small new water input. Water chemistry data imply some new water input during the second hydrograph response. Without a prestorm sample, both Cl and EC fluctuations are difficult to quantify, but it appears that dilution of M8 Cl and EC concentrations occurred immediately following peak flow at 1400 LT on November 27. Cl concentration returned to a preresponse value (3.8 ppm) after deflection toward rain Cl, but dilute M8 EC concentrations persisted for the duration of the event.

Pit A throughflow peak (600 mL min^{-1}) coincided with the second streamflow peak, while pit 5 throughflow peak (3000 mL min^{-1}) lagged pit A by 12 hours (Figure 5). Pit A showed a relatively large δD deflection from prestorm δD (−37‰) toward rain δD, and peak new water input reached 25%, using a two-component model with nearby suction lysimeter water as C_o, drum flow as C_s and rainfall as C_n. Pit A water chemistry showed large increases in Cl concentration and EC, indicating increased total solute concentration. Although both of these shifts were away from rain chemistry values, they may indicate the flushing of high Cl and solute-rich soil water, which had been enriched possibly during evaporative conditions preceding the event. Pit 5 throughflow δD showed approximately 14% new water at peak flow, employing the same technique used for pit A. Pit 5 water chemistry showed very little change through the event and mirrored M8 Cl and EC concentrations.

Soil Water and Groundwater Isotopic Distribution

Suction lysimeter (SL) δD results for the 4-month period in which the episodes described above occurred are shown by *Stewart and McDonnell* [1991, Figure 3]. All SL sites (Table 4) showed a somewhat dampened response to the sinusoidal high-amplitude rain δD input, but varied according to their slope position and depth within the profile. Generally, shallow SLs and those installed near the watershed divide (i.e., SL4, SL6, SL7) showed the highest amplitude shifts with bulk storm rainfall, but with significant time lags in peaks. On the other hand, those SLs installed at depth, or near the valley bottom (e.g., SL2, SL8, SL9) showed a highly dampened and lagged response to bulk storm rainfall, and more closely resemble M8 base flow time series. These long-term relationships are described in detail by *Stewart and McDonnell* [1991].

To quantify the description of SL δD response through time and to reinforce any spatial trends in the data (i.e., downslope or with increasing depth), a simple multivariate cluster analysis [*Everitt*, 1974] was performed using the data shown in the work by *Stewart and McDonnell* [1991]. The relationships between each SL site are depicted in Figure 6 in the form of phenograms, based on the nearest neighbor Euclidean distance method [*Systat*, 1985]. Three groups can be detected: SL5, SL10, SL6 and then SL3 (group A) amalgamated at the shortest distance and are therefore the most similar sites, SL8, SL9 and SL11 (group B) joined shortly after group A and show some spatial correlation with group A after half distance. SL7 and SL4 (group C) show no spatial correlation to groups A or B, but remain isolated throughout the entire distance and form a distinct grouping.

The quantitative groupings established by the cluster analysis are consistent with the model description of δD trends in the work by *Stewart and McDonnell* [1991]. Group A seems to represent a midslope, midprofile location, in which suction lysimeter δD response is intermediate between both high- and low-amplitude sites. Group B is more representative of a near-stream site, or deep SL in a slope hollow. This group would maintain the lowest amplitude of response, and also the longest lag between rain input and SL

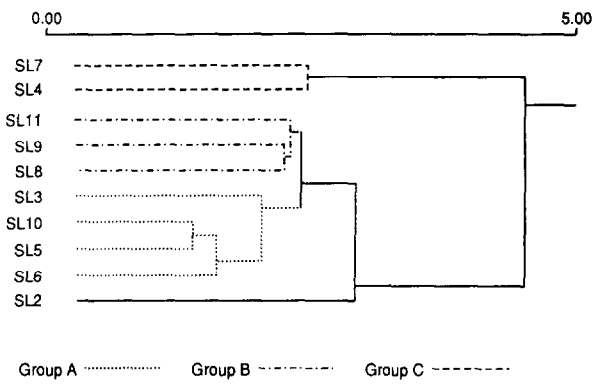

Fig. 6. Phenogram showing relationships between SL sites for the September 7 to December 16 period, using the standard distance coefficient.

and δD shift. Group C is clearly a shallow soil zone: one with a large amplitude in δD values through time, similar to the rainfall δD input. Daily SL and rainfall δD values are plotted in Figure 7.

The November 26–27 rain event was sampled intensively to examine the SL δD response on an event time scale. This was also done to see whether longer-term groupings (Figure 6) persisted and whether large within-storm soil water or groundwater δD shift occurred. Because suction lysimeter samples were extracted on an irregular time series (i.e., during daylight hours within a 0800–1800 LT working day) and filled at varying rates (~1–5 hours) and because weighted mean rain δD was computed for 2400–2400 LT periods, some error was introduced into the lag response. Nevertheless, some general comments and trends can be outlined.

Phenograms for the daily time series are shown in Figure 8, and indicate that although the rates of amalgamation shifted, groups identified in the weekly time series remained intact. SL9 was an exception to this pattern and moved from group B into group A. SL3, SL9, SL10, SL6 and SL5 (in that order) amalgamated first and therefore maintained the closest similarity. These values remained relatively unchanged isotopically through the period. SL4 and SL7 (group C) showed the highest δD fluctuations, in response to rain δD input. Daily rainfall δD values are shown in Figure 7. Rain δD shifted from −72.9‰ to a peak of −40.4‰ (November 28), before dropping to circa −112‰. Group C values

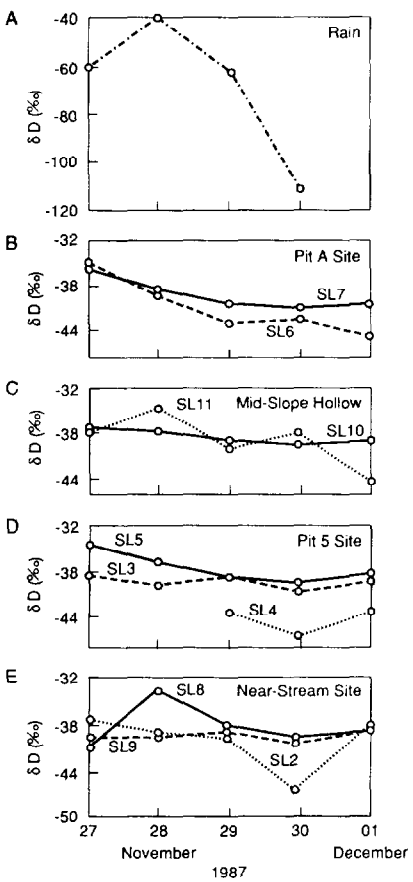

Fig. 7. Variations in rainfall and SL δD concentrations for the November 27 to December 1 period.

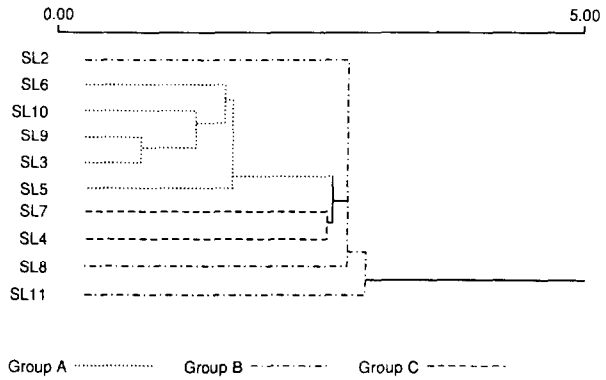

Fig. 8. Phenogram showing relationships between SL sites for the November 27 to December 1 period, using the standard distance coefficient.

showed decreasing δD through time, but did not show any sensitivity to large variations observed in rain signal. Part of this may be due to the fact that rain δD shifted very close to the prestorm SL4 and SL7 value, negating SL δD response. Nevertheless, a trend toward rain δD was apparent, indicating substantial new water in the shallow soil zone (<25 cm). Group B sites (SL8 and SL11) were again intermediate between both group A and group B, in terms of the amplitude of response to rain δD. In this case, however, SL8 and SL11 shifted away from the rain signal on November 28, and then returned to a constant unchanged signal for the rest of the event. This initial movement may be a result of heavier (less negative) water being displaced downward through the profile, in response to the initial wetting front caused by the rainfall burst. The δD values from shallow soil locations seem to confirm this postulation (i.e., SL7 = −35‰).

DISCUSSION

Stream Episodic Response

The 11 monitored 1987 storms showed little new water flushing (0–25%), and in many cases stream deuterium concentrations (C_s) following the onset of rainfall (C_n) did not escape mass spectrometer experimental error. This situation resulted in relatively higher uncertainty associated with hydrograph separation. The choice of prestorm concentrations (C_o) has a large impact on estimates of the Q_o/Q_n ratio. For example, Figure 9 shows how the standard two-component model is affected by a ±1‰ change in C_o. Although most old water estimates are with ±5% of the original value, considerable uncertainty is introduced for the sample at peak flow on November 26 (Figure 9) because of the unrealistic value of C_o.

If the three-component model (equation (4)) is used, the possibility for uncertainty increases again because of shifting values of C_s and C_{gw}. Suction lysimeter samples extracted over a 5-day period in Figure 7 showed that both soil water and (to a lesser extent) groundwater shifted their δD signatures within an event. Therefore, any assumptions of static preevent old water components are unrealistic for this watershed and likely other steep humid catchments. The choice of C_s and C_{gw} values to be entered into (4), a priori, is highly problematic.

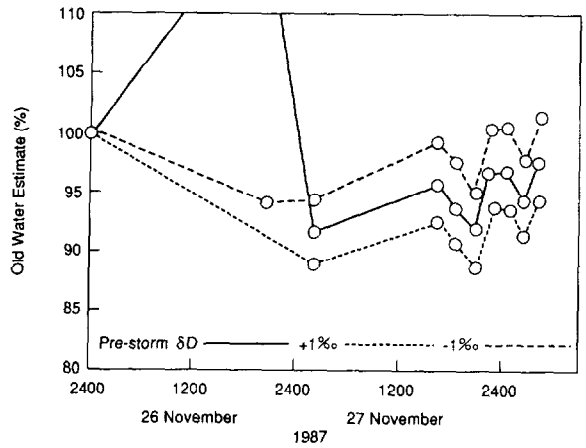

Fig. 9. Two-component old water estimates using C_o and $\pm 1‰$ C_o.

Between-Storm Subsurface Mixing of Old Water

Under low-flow (base flow) conditions, M8 streamflow is sustained by slow continual unsaturated downslope drainage toward the channel from midslope and upslope zones. This would also include a thin (<10 mm) layer of saturated drainage at the mineral soil–Old Man Gravel interface. Local catchment characteristics such as steep sideslopes, shallow soils, incised valley bottoms with little aquifer storage, and impermeable underlying bedrock augment this process and result in the continual priming of near-stream zones with older water. This is evident in the long-term suction lysimeter data from *Stewart and McDonnell* [1991]. Tensiometer evidence [*McDonnell*, 1990] showed that soil moisture content increases downslope, such that saturated or near-saturated conditions occur regularly in the near-stream zone (cf. near-stream tensiometer data). This constant downslope movement between storms produces two key features of stream episodic response: (1) hydrograph rise and the timing of channel response is accelerated because the near-stream zone is so well-primed, and (2) the age of subsurface water increases considerably downslope (see model results of *Stewart and McDonnell* [1991]) so that large old water volumes are in a discharge position and ready for quick displacement into the channel.

The process of continual downslope mixing and progressive displacement of subsurface water has been outlined by *Horton and Hawkins* [1965] and *Zimmerman et al.* [1966]. From laboratory experiments using tritiated water, both studies showed that drainage from the upslope zone in sloping soil profiles displaced downslope soil water. Although all suction lysimeter sites showed a somewhat dampened response to the sinusoidal high-amplitude rain δD input, each varied according to slope position and depth within the soil profile. Exponential modeling results from *Stewart and McDonnell* [1991] showed that mean age increased downslope, so that water in the near-stream zone was >100 days old, while that in upslope zones was roughly 2 weeks old. Theoretically, if soil water from upslope zones (with discrete δD values) drains into the midslope zone and then into the near-stream zone, as proposed by the exponential model, then the long-term average δD of each site must be the same (disregarding the 1–100 day lag for water to move from the ridge to the channel). Suction lysimeter δD for all sites, averaged over the complete period, was −39.9‰ (s.d. = ±1.4‰). All individual site averages, including M8 base flow, were within ±1‰ of the mean value. Because of persistent rainfall during this period, evaporation was limited within the watershed.

Within-Storm Subsurface Mixing of Old Water

In steep catchments, three-dimensional topographic convergence of subsurface flow exerts a strong influence on hillslope runoff production. Several studies [*Beven*, 1978; *O'Loughlin*, 1981; *Beven et al.*, 1988] have shown that convergent zones may yield earlier and higher peak subsurface flows than planar of convex slope segments. *Anderson and Burt* [1978] noted that in a catchment with 25° slope angles and 1.5–2.0 m deep soils, nose slope contributions per meter of channel length per square meter drained area were almost an order of magnitude less than hollow contributions. Although spur reaches along the stream composed 60% of the basin area, *Anderson and Burt* [1978] noted that these zones only contributed 40% of the total discharge under the most favorable of conditions.

In the M8 catchment, up to 75% of the total channel length is fed by either planar sideslope zones or nose slopes. The catchment itself, however, is strongly dissected, and hollow zones and sideslopes draining into hollow zones compose roughly 85% of the total catchment area. Some comparison between hollow, nose or planar slope runoff volumes and timing can be gathered from data presented by *Mosley* [1979]. He showed a large difference between quick flows from pit 1 and pit A, which are only 4 m apart. Pit 1 is on a planar slope with a 0.2-m-deep soil cover, whereas the catchment area of pit A (used in this study) is bowl shaped, and the soil is 0.45 m deep. Mosley also determined regression relationships between peak specific discharge in L s^{-1} ha^{-1} at the main weir and at the pit 1 and pit A sites:

$$Q_m = 0.799 Q_{1\ 0.82} \qquad r^2 = 0.92 \tag{8}$$

$$Q_m = 1.98 Q_{A\ 0.54} \qquad r^2 = 0.83 \tag{9}$$

where Q_m, Q_1 and Q_A are the discharge at the main weir, pit 1 and pit A, respectively. For several storms during 1978, equality was attained at

$$Q_m = Q_1 = 0.3 \text{ L s}^{-1} \text{ ha}^{-1} (1.15 \text{ L s}^{-1}) \tag{10}$$

$$Q_m = Q_A = 1.42 \text{ L s}^{-1} \text{ ha}^{-1} (5.45 \text{ L s}^{-1}) \tag{11}$$

where the value in parentheses is the discharge at the M8 weir.

These relationships show that pit A produces quick flow at smaller quantities than the main weir, when the latter is less than 10 mm. Furthermore, pit 1 quick flow volumes are higher than pit A for small events, because of thinner and more permeable soils. For a 17-mm rain event, *Mosley* [1979] showed that quick flow at the main weir, pit 1 and pit A were 1.9, 2.6, and 0.2 mm, respectively. For larger events (>10 mm quick flow), pit A quick flow depth exceeded both pit 1 and M8. This suggests two important factors: (1) for small events, hillslope flow does not significantly account for channel storm flow, and this is verified by computations made by *McDonnell* [1990], and (2) hollows dominate runoff production during high flow.

Although not stated explicitly in previous investigations [e.g., *Sklash et al.*, 1986], topographic convergence of subsurface water into hollows will have a strong influence on

soil water and groundwater isotopic mixing. If one accepts that hillslope hollows dominate channel storm flow in moderate to large events, then they must also control resulting streamflow isotopic compositions. Suction lysimeter data demonstrated large δD differences between shallow (SL4) and deep (SL3) zones and ridge (possible SL7) and hollow zones (possible SL6). In addition to mixing at a point during an event, hollow zones receive new water from surrounding slope segments, which mixes with older hollow water before being transmitted to the channel.

CONCLUSIONS

Deuterium concentrations in old water components (soil water and groundwater) vary markedly in time and space in the Maimai M8 catchment, both within and between rainfall episodes. Because of the relatively short residence time of water in the catchment, small differences in the C_o term alter Q_o/Q_n ratio considerably. Statistical analysis of streamflow samples showed that ±2‰ represented a significant difference in deuterium values between successive samples. Of the 11 sampled rainfall events, only four events demonstrated new water flushing where episodic stream deuterium composition deflected >2‰ from prestorm values. Analysis of the November 26–28 event (47 mm rainfall, 9.8 mm runoff) showed that old water dominated channel storm flow by 90% using a standard two-component hydrograph separation for deuterium. Three-component hydrograph separation indicated that 12–16% was in the form of soil water, with <5% as on-channel precipitation and 80% groundwater. Soil water and groundwater deuterium concentrations showed systematic trends both in a downslope and downprofile direction.

Between-storm suction lysimeter deuterium data illustrated a dampened response to high-amplitude rainfall deuterium concentrations. Three distinct soil water/groundwater groupings were identified with respect to soil depth and geographic position within the watershed. Within-storm suction lysimeter sampling preserved similar groupings, indicating that the subsurface reservoir is poorly mixed on the time scale of hours to days. Topography controlled mixing to a large extent, both within and between events. Within-storm variation in C_s and C_o is difficult to determine because of rapid shifts in water table associated with soil water pathways. Uncertainty/sensitivity analyses are currently under way for the two- and three-component models using the Maimai data and other available data sets. It is hoped that the results will identify conditions and locations under which isotopic separations are ill-advised, due to spatial and temporal variability of rain, soil and groundwater concentrations. If water samples are sufficient in time and space, a time series approach [*Turner et al.*, 1987; *Stewart and McDonnell*, 1991] may be most applicable to flow component identification in small watersheds.

Acknowledgments. J.J.M. would like to thank the following organizations for their support: American Geophysical Union Horton Research Grant, New Zealand Commonwealth Scholarship and Fellowship Programme, University Grants Committee and the University of Canterbury Geography Department. I.F.O. would like to thank the University Grants Committee and the University of Canterbury. The Institute of Nuclear Sciences and Forest Research Centre are also thanked for their analytical services and logistical support throughout the study. J. Buttle, R. Sidle, and C. Taylor are thanked for their comments on an earlier draft of the manuscript. J. Gray is thanked for the water chemistry analysis. This research was supported by the Utah Experiment Station, Utah State University, Logan. Approved as journal paper 4221.

REFERENCES

American Public Health Association, *Standard Methods for the Examination of Water and Waste Water*, 14th ed., 1193 pp., Washington, D. C., 1976.

Anderson, M. G., and T. P. Burt, Toward a more detailed field monitoring of variable source area, *Water Resour. Res.*, *14*, 1123–1131, 1978.

Beven, K., The hydrological response of headwater and sideslope areas, *Hydrol. Sci. Bull.*, *23*, 419–437, 1978.

Beven, K., E. F. Wood, and M. Sivapalan, On hydrological heterogeneity: Catchment morphology and catchment response, *J. Hydrol.*, *100*, 353–375, 1988.

Coleman, M. L., T. J. Shepherd, J. J. Durham, J. E. Rouse, and G. R. Moore, Reduction of water with zinc for hydrogen isotope analysis, *Anal. Chem.*, *54*, 993–995, 1982.

Craig, H., Isotope variations in meteoric waters, *Science*, *133*, 1702–1703, 1961.

DeWalle, D. R., B. R. Swistock, and W. E. Sharpe, Three component tracer model for stormflow on a small Appalachian forest catchment, *J. Hydrol.*, *104*, 301–310, 1988.

Everitt, B. S., *Cluster Analysis*, Heinemann Educational Books, London, 1974.

Hewlett, J. D., and A. R. Hibbert, Factors affecting the response of small watersheds to precipitation in humid areas, in *International Symposium on Forest Hydrology*, edited by W. E. Sopper and W. H. Lull, pp. 275–290, Pergamon, New York, 1967.

Horton, J. H., and R. H. Hawkins, Flow path of rain from the soil surface to the water table, *Soil Sci.*, *100*, 377–383, 1965.

McDonnell, J. J., A rationale for old water discharge through macropores in a steep, humid catchment, *Water Resour. Res.*, *26*, 2821–2983, 1990.

McDonnell, J. J., M. Bonell, M. K. Stewart, and A. J. Pearce, Deuterium variations in storm rainfall: Implications for stream hydrograph separations, *Water Resour. Res.*, *26*, 455–458, 1990.

Mosley, M. P., Streamflow generation in a forested watershed, New Zealand, *Water Resour. Res.*, *15*, 795–806, 1979.

O'Loughlin, E. M., Saturated regions in catchments and their relations to soil and topographic properties, *J. Hydrol.*, *53*, 229–246, 1981.

Pearce, A. J., M. K. Stewart, and M. G. Sklash, Storm runoff generation in humid headwater catchments, 1, Where does the water come from?, *Water Resour. Res.*, *22*, 1263–1271, 1986.

Pionke, H. B., J. R. Hoover, R. R. Schnabel, W. J. Gburek, J. B. Urban, and A. S. Rogowski, Chemical-hydrologic interactions in the near-stream zone, *Water Resour. Res.*, *24*, 1101–1110, 1988.

Seip, H. M., D. O. Anderson, N. Christophersen, T. J. Sullivan, and R. D. Vogt, Variations in concentrations of aqueous aluminum and other chemical species during hydrological episodes at Birkenes, southernmost Norway, *J. Hydrol.*, *108*, 387–405, 1989.

Sklash, M. G., M. K. Stewart, and A. J. Pearce, Storm runoff generation in humid headwater catchments, 2, A case study of hillslope and low-order stream response, *Water Resour. Res.*, *22*, 1273–1282, 1986.

Stewart, M. K., and J. J. McDonnell, Modeling baseflow soil water residence times from deuterium concentrations, *Water Resour. Res.*, *27*, 2682–2693, 1991.

Systat, *Software Manual*, 417 pp., Evanston, Ill., 1985.

Turner, J. V., D. K. Macpherson, and R. A. Stokes, The mechanisms of catchment flow processes using natural variations in deuterium and oxygen-18, *J. Hydrol.*, *94*, 143–162, 1987.

Zimmerman, U., K. O. Munnich, W. Roether, W. Kreutz, K. Schubach, and O. Siegel, Tracers determine movement of soil moisture and evapotranspiration, *Science*, *152*, 346–347, 1966.

J. J. McDonnell, Watershed Science Unit, Department of Forest Resources, Utah State University, Logan, UT 84322.

I. F. Owens, Department of Geography, University of Canterbury, Christchurch, New Zealand.

M. K. Stewart, Institute of Nuclear Sciences, Department of Scientific and Industrial Research, Lower Hutt, New Zealand.

(Received March 4, 1991;
revised July 26, 1991;
accepted July 30, 1991.)